Influence of Uniaxial Loads on Local Resonances

KEPING ZHANG, YUNING WU, RANTING CUI
and XUAN ZHU

ABSTRACT

Accurate and reliable nondestructive evaluation (NDE) for stress measurement is essential for assessing structural performance and preventive maintenance. Local resonances offer an efficient NDE method due to their "amplified and localized" vibration amplitude. This allows for mounting or wiring near the structural edge without affecting the vibration modes. In this paper, we investigate the influence of stress level on the local resonances in a rectangular aluminum bar structure. In the first step, we utilize the electromechanical impedance method (EMI) to extract local resonances and verified them as Zero-Group-Velocity (ZGV) mode and cutoff frequency modes by performing two-dimensional fast Fourier transform (2D-FFT) on the wavefield. Furthermore, we investigate the influence of uniaxial tensile stress on the local resonance frequencies. It is observed that both the ZGV mode and cutoff frequency mode demonstrate a measurable sensitivity to the applied axial load.

Keping Zhang, Yuning Wu, Ranting Cui, Xuan Zhu, Dept. of Civil & Environmental Engineering, University of Utah, 110 Central Campus Dr., Salt Lake City, UT 84112, U.S.A.

INTRODUCTION

Local resonances phenomena have gained the interest of researchers due to their energy-trapping and dominant resonance in amplitude spectra [1]. Various studies have been conducted to observe local resonances in waveguide structures such as plate [2], [3], bar [4], [5], cylinder [6], and rail [7]. The results have shown that the resonance is related to the zero group velocity (ZGV) point or cutoff frequency point [5]. At these points, group velocity decrease to zero, resulting in a vanished wave energy velocity, thereby wave energy cannot propagate away. The ZGV mode and cutoff frequency mode exhibit different wavelength phenomenon, with a non-zero wavenumber at ZGV mode and a zero wavenumber at cutoff frequency mode [8]. These modes offer an efficient tool for nondestructive evaluation (NDE) applications, such as defect detection [9], material properties estimation [1], and thickness evaluation [10], [11].

However, stress measurement based on the local resonances has not been explored. Most of studies have relied on propagating guided waves and their time-of-flight calculation for stress measurement [12]–[14], which has encountered challenges in accurately measuring wave speed due to inadequate variation. In this study, we experimentally investigate the influence of uniaxial stress level on the local resonances in terms of local resonance frequencies shift measured by electromechanical impedance method (EMI). In the following sections, we first identified ZGV and cutoff modes frequencies from dispersion curves of a rectangular aluminum bar using eigenanalysis study in COMSOL software. We then adopted EMI method for both excitation and measurement, dominant resonance frequencies were observed from EMI conductance spectra. Furthermore, we performed two-dimensional fast Fourier Transform (2D-FFT) analysis to identify these resonances as ZGV and cutoff frequencies modes in the wavenumber-frequency spectra. Additionally, the wave profile measured by laser vibrometer demonstrates the energy-trapping phenomenon at both ZGV mode and cutoff frequencies mode, allowing for mounting at the far field structural edges for a tensile loading test without affecting modes. In the last section, we conducted the uniaxial tensile loading test to study the effect of stress level on the local resonance frequencies. The results demonstrates that local resonance frequency variation caused by changes in stress level can be accurately measured by EMI.

LOCAL RESONANCE GENERATION AND 2D-FFT ANALYSIS

The studied structure is a rectangular aluminum bar with 25.4 mm width, 6.35 mm thickness, and 1 m length. First, we calculated the dispersion curves over the rectangular cross-section by eigenfrequencies analysis of a unit cell in COMSOL Multiphysics . The Bloch-Floquet periodic boundary condition with a predefined wavenumber (k) was assigned to the wave propagation direction of the unit cell as indicated in Figure 1(a). A quarter of the unit cell was simulated with symmetric or antisymmetric boundary conditions to identify four mode families: Longitudinal (L), Flexural Vertical (FV), Flexural Horizontal (FH), and Torsional (T) modes. The nominal material properties of 6063 aluminum alloy were adopted: Young's modulus E = 69 GPa, Poisson's ratio v = 0.33, and density 2700 kg/m^3. The unit cell was meshed using cubic elements with a mesh size of 1 mm. The wavenumber k was swept from 0 to 30 1/m. Figure 1(b) shows the calculated dispersion curves from 0 to 200 kHz.

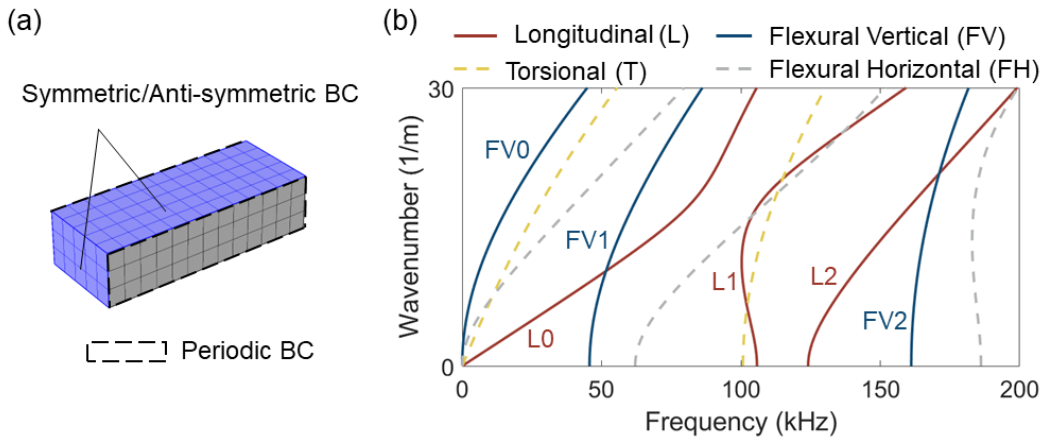

Figure 1. (a) A meshed unit cell indicating the boundary conditions, and (b) dispersion curves.

By the principle of EMI, a piezoelectric patch was attached to the middle of the top surface of the aluminum bar, providing broadband excitation ranging from 10 to 200 kHz, then the structural resonance frequencies can be identified from the PZT generated electric conductance spectra [15]. Additionally, these resonance modes were further identified through 2D-FFT analysis and visualized using recorded velocity along the wave propagation direction. The detailed simulation and experimental setup were discussed in our previous work, and the results for both agree well with each other [6]. Here, we presented the experimental conductance spectra and frequency-wavenumber (f-k) spectra as shown in Figure 2. The conductance spectra illustrate four resonances at frequencies of 46.2 kHz, 100.7 kHz, 105.3 kHz, and 161.6 kHz in Figure 2(a). Figure 2(b) shows the f-k spectra overlapped with calculated dispersion curves (red dashed lines). The highlight excited branches in f-k spectra align well with the dispersion curves, therefore, identify the four resonances in conductance spectra as FV1-cutoff at 45.51 kHz, L1-ZGV at 99.68 kHz, L1-cutoff at 105.2 kHz, and FV2-cutoff at 160.12 kHz, respectively. The slight frequency difference between conductance spectra and f-k spectra were also observed in [16], [17].

To further investigate wave propagation pattern at local resonance frequencies, a velocity scan using 3D laser vibrometer was performed along the wave propagation direction on surface opposite the attached PZT. Figure 3 is the experiment setup. The scan started 10 mm away from the PZT center. To improve the surface optical condition, 3M 7610 retroreflective tape was mounted on the surface of the aluminum bar [18]. Modeling clay was put around bar edges to eliminate boundary reflection interference. By Fourier transforming the time signal to frequency spectra, velocity map around FV1-cutoff and L1-ZGV frequencies were obtained.

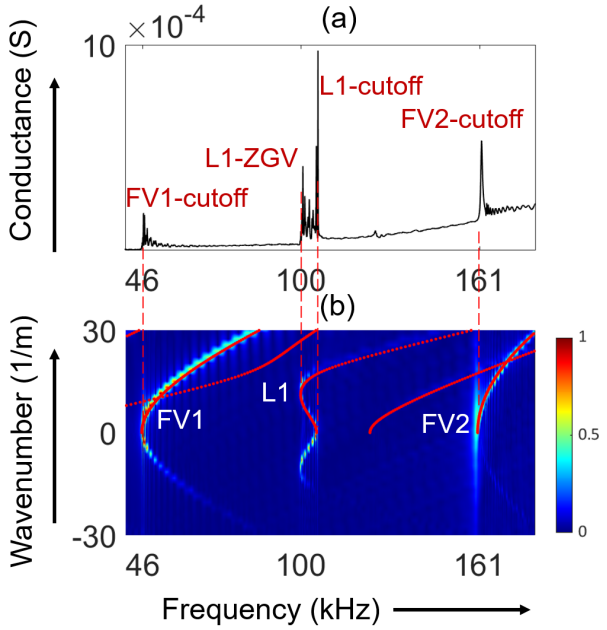

Figure 2. Experimental results: (a) conductance spectra (b) dispersion relations in *k-f* domain.

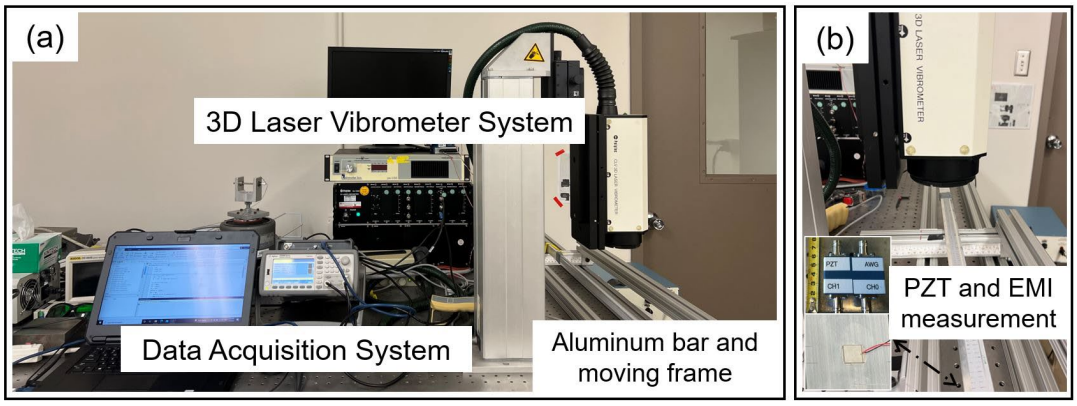

Figure 3. Experimental setup for wave profile measurement.

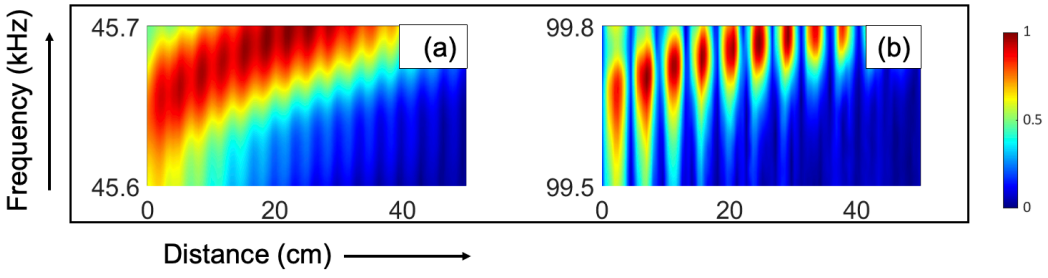

Figure 4. Experimental velocity map (a) FV1-cutoff mode, (b) L1-ZGV mode.

Figure 4 shows the experimental wave profiles around FV1-cutoff and L1-ZGV frequencies. The energy-trapping feature is observed close to the source location at the minimum cutoff and ZGV frequencies, respectively. For L1-ZGV mode, it is also observed that a standing wave pattern with the wavelength approximate 10 cm due to the interference of two propagating waves in opposite directions as shown Figure 3(b).

INFLUENCE OF UNIAXIAL STRESS ON LOCAL RESONANCES

Our previous studies have demonstrated that the local resonances are immune to far field boundary conditions. This finding allows for mounting or wiring near the structural edge without affecting the vibration modes, and offers the possibility of quantitatively evaluating the stress level by measuring the resonance frequency shift directly in the EMI spectra. In this section, we investigate the influence of uniaxial stress level on local resonance frequencies. Figure 4 shows the experimental setup, which employs an EMI measurement system and an Instron 5659 Testing System. A strain gauge was also attached to the aluminum bar and connected to a strain indicator (Vishay P-3500) to control the tensile load level. The tensile strain was linearly increased from 0 to 1500 macrostrain in 16 steps, corresponding to a maximum tensile stress of 103.5 MPa. For each loading step, an EMI test was conducted to collect resonant frequencies.

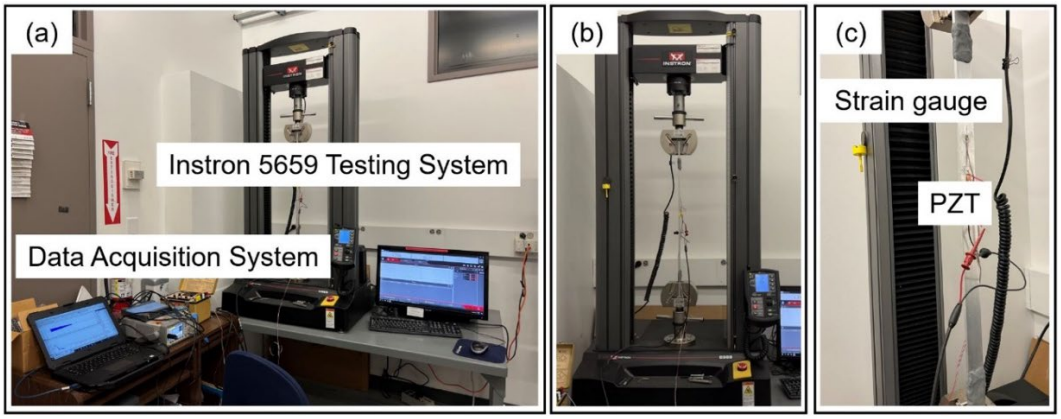

Figure 5. Uniaxial tension loading test setup.

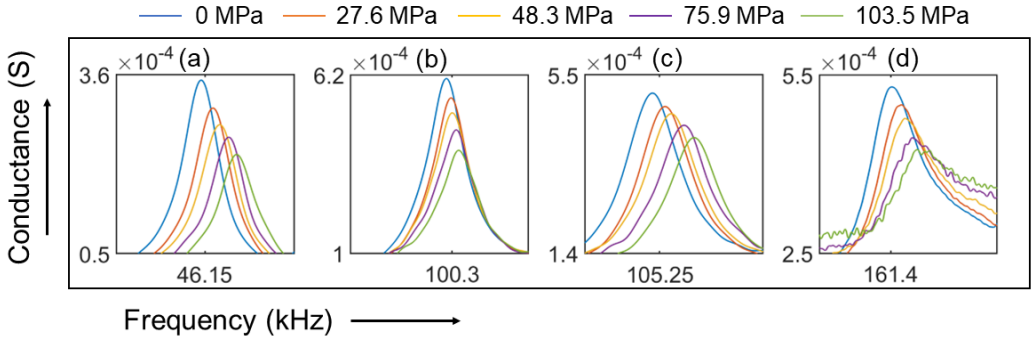

Figure 6. Variation in the four local resonances under the uniaxial tensile stress (a) FV1-cutoff, (b) L1-ZGV, (c) L1-cutoff, and (d) FV2-cutoff modes.

As shown in Figure 6, the resonance frequency of the FV1-cutoff, L1-ZGV, L1-cutoff, and FV2-cutoff modes increases with increasing tensile stress. Moreover, it can be observed that the resonance amplitude in the conductance spectra decreases as the tensile stress level increases. This is because the tensile load causes a reduction in stiffness, resulting in smaller conductance [13]. Sensitivity (Hz/MPa) was defined as the frequency shift verse stress for quantitively analysis. Calculated sensitivity based on experimental results is 0.64 Hz/MPa for FV1-cutoff, 0.41 Hz/MPa for L1-ZGV, 0.93 Hz/MPa for L1-cutoff, and 2.57 Hz/MPa for FV2-cutoff. The most sensitive mode to stress is FV2-cutoff, while the least sensitive one is the L1-ZGV mode.

CONCLUSTION

In summary, we investigated the unique features of local resonance, such as energy-trapping and minimum frequency behavior, and studied the effect of uniaxial stress on the local resonance frequencies. Our experimental results indicate that FV2-cutoff is the most sensitive mode to tensile stress, with a sensitivity of 2.57 Hz per MPa, while L1-ZGV was the least sensitive, with a sensitivity of 0.41 Hz per MPa. These variations could be accurately measured by EMI.

ACKNOWLEDGEMENTS

This work was supported by the U.S. Department of Energy NEUP Project 2124288. This work was also partially funded by the University of Utah startup package. The support and resources from the Center for High Performance Computing at the University of Utah are gratefully acknowledged.

REFERENCES

[1] C. Prada, D. Clorennec, and D. Royer, “Local vibration of an elastic plate and zero-group velocity Lamb modes,” *J. Acoust. Soc. Am.*, vol. 124, no. 1, pp. 203–212, Jul. 2008, doi: 10.1121/1.2918543.

[2] D. Clorennec, C. Prada, and D. Royer, “Local and noncontact measurements of bulk acoustic wave velocities in thin isotropic plates and shells using zero group velocity Lamb modes,” *J. Appl. Phys.*, vol. 101, no. 3, p. 034908, Feb. 2007, doi: 10.1063/1.2434824.

[3] A. Gibson and J. S. Popovics, “Lamb wave basis for impact-echo method analysis,” *J. Eng. Mech.*, vol. 131, no. 4, pp. 438–443, 2005.

[4] J. Laurent, D. Royer, and C. Prada, “In-plane backward and zero group velocity guided modes in rigid and soft strips,” *J. Acoust. Soc. Am.*, vol. 147, no. 2, pp. 1302–1310, Feb. 2020, doi: 10.1121/10.0000760.

[5] K. Zhang, R. Cui, Y. Wu, L. Zhang, and X. Zhu, “Extraction and selective promotion of zero-group velocity and cutoff frequency resonances in bi-dimensional waveguides using the electromechanical impedance method,” *Ultrasonics*, vol. 131, p. 106937, May 2023, doi: 10.1016/j.ultras.2023.106937.

[6] V. Damljanović and R. L. Weaver, “Propagating and evanescent elastic waves in cylindrical waveguides of arbitrary cross section,” *J. Acoust. Soc. Am.*, vol. 115, no. 4, pp. 1572–1581, Apr. 2004, doi: 10.1121/1.1687424.

[7] Y. Wu, R. Cui, K. Zhang, X. Zhu, and J. S. Popovics, “On the existence of zero-group velocity modes in free rails: Modeling and experiments,” *NDT E Int.*, vol. 132, p. 102727, 2022.

[8] C. Grünsteidl *et al.*, "Measurement of the attenuation of elastic waves at GHz frequencies using resonant thickness modes," *Appl. Phys. Lett.*, vol. 117, no. 16, p. 164102, Oct. 2020, doi: 10.1063/5.0026367.
[9] S. D. Holland and D. E. Chimenti, "Air-coupled acoustic imaging with zero-group-velocity Lamb modes," *Appl. Phys. Lett.*, vol. 83, no. 13, pp. 2704–2706, Sep. 2003, doi: 10.1063/1.1613046.
[10] M. Cès, D. Clorennec, D. Royer, and C. Prada, "Thin layer thickness measurements by zero group velocity Lamb mode resonances," *Rev. Sci. Instrum.*, vol. 82, no. 11, p. 114902, Nov. 2011, doi: 10.1063/1.3660182.
[11] O. Baggens and N. Ryden, "Systematic errors in Impact-Echo thickness estimation due to near field effects," *NDT E Int.*, vol. 69, pp. 16–27, Jan. 2015, doi: 10.1016/j.ndteint.2014.09.003.
[12] M. Lematre, G. Feuillard, T. Delaunay, and M. Lethiecq, "Modeling of ultrasonic wave propagation in integrated piezoelectric structures under residual stress," *IEEE Trans. Ultrason. Ferroelectr. Freq. Control*, vol. 53, no. 4, pp. 685–696, 2006.
[13] F. Chen and P. D. Wilcox, "The effect of load on guided wave propagation," *Ultrasonics*, vol. 47, no. 1–4, pp. 111–122, Dec. 2007, doi: 10.1016/j.ultras.2007.08.003.
[14] M. I. Albakri, V. V. N. S. Malladi, and P. A. Tarazaga, "Low-frequency acoustoelastic-based stress state characterization: Theory and experimental validation," *Mech. Syst. Signal Process.*, vol. 112, pp. 417–429, Nov. 2018, doi: 10.1016/j.ymssp.2018.04.011.
[15] C. Liang, F. Sun, and C. A. Rogers, "Electro-mechanical impedance modeling of active material systems," *Smart Mater. Struct.*, vol. 5, no. 2, p. 171, 1996.
[16] S. Opoka, P. Malinowski, T. Wandowski, L. Skarbek, and W. Ostachowicz, "Damage detection using electromechanical impedance technique combined with scanning laser vibrometry," presented at the Key Engineering Materials, Trans Tech Publ, 2013, pp. 687–694.
[17] Q. Zhang, S. Shi, and W. Chen, "An electromechanical coupling model of a longitudinal vibration type piezoelectric ultrasonic transducer," *Ceram. Int.*, vol. 41, pp. S638–S644, 2015.
[18] M. Hasanian and C. J. Lissenden, "Assessment of coating layers on the accuracy of displacement measurement in laser Doppler vibrometry," presented at the AIP Conference Proceedings, AIP Publishing LLC, 2017, p. 050006.
[19] C.-W. Ong, Y. Yang, A. S. K. Naidu, Y. Lu, and C. K. Soh, "Application of the electromechanical impedance method for the identification of in-situ stress in structures," presented at the Smart Structures, Devices, and Systems, SPIE, 2002, pp. 503–514.